Double walled carbon nanotubes promote the overproduction of extracellular protein-like polymers in Nitzschia palea: An adhesive response for an adaptive issue

Laurent Verneuil, Jérôme Silvestre, Irina Randrianjatovo, Claire-Emmanuelle Marcato-Romain, Elisabeth Girbal-Neuhauser, Florence Mouchet, Emmanuel Flahaut, Laury Gauthier, Eric Pinelli

Double walled carbon nanotubes promote the overproduction of extracellular protein-like polymers in *Nitzschia palea*: An adhesive response for an adaptive issue

Laurent Verneuil [a,b], Jérôme Silvestre [a,b,c], Irina Randrianjatovo [d], Claire-Emmanuelle Marcato-Romain [d], Elisabeth Girbal-Neuhauser [d], Florence Mouchet [a,b,c], Emmanuel Flahaut [c,e,f], Laury Gauthier [a,b,c], Eric Pinelli [a,b,c,]*

[a] EcoLab (Laboratoire d'Ecologie Fonctionnelle et Environnement), ENSAT, INP, UPS, Université de Toulouse, UMR CNRS 5245, Castanet Tolosan, France

[b] CNRS, EcoLab, Castanet Tolosan, France

[c] Laboratoire Commun NAUTILE (CNRS, UPS, INPT, ARKEMA), Laboratoires EcoLab, CIRIMAT, GRL, France

[d] LBAE (Laboratoire de Biotechnologies Agro-alimentaire et Environnementale), Université de Toulouse, UPS EA 4565, Institut Universitaire de Technologie, 24 Rue d'Embaquès, 32000 Auch, France

[e] Institut Carnot CIRIMAT (Centre Inter-Universitaire de Recherche et d'Ingénierie des Matériaux), Université de Toulouse, INP, UPS, UMR CNRS 5085, Toulouse, France,

[f] CNRS, Institut Carnot CIRIMAT, Toulouse, France

ABSTRACT

The present study assessed the effects of double-wall carbon nanotubes (DWCNTs) dispersed in the presence of a realistic concentration of natural organic matter (NOM, 10 mg L^{-1}) on the benthic diatom *Nitzschia palea* using toxicity tests and quantitative/qualitative extracellular polymeric substances (EPS) assays. No toxic effect was observed. A growth delay was measured after 48 h of exposure to concentrations of DWCNTs ranging from 1 mg L^{-1} (~29%) to 50 mg L^{-1} (~84%). Extracellular carbohydrates and proteins were extracted using a sequential multi-methods protocol to collect soluble, hydrophobic and ion-bridged extracellular polymeric substances (EPS). Extracted EPS were analyzed by colorimetric assays and size exclusion chromatography. The results highlighted a higher EPS concentration in exposed cultures that was primarily caused by an overproduction of protein-like polymers (protein or glycoproteins, PLPs). Such EPS overproduction and increase in proteins/carbohydrates ratio can partially explain the observed growth inhibition. EPS were preferentially extracted using hydrophobic conditions and were mainly composed of PLPs with either low (10 kDa) or high (174 kDa) molecular weights. These data highlights the affinity between DWCNTs and EPS, which is primarily driven by both physical and hydrophobic interactions. This indicates that *N. palea* can respond to DWCNTs by forming an EPS network optimized for adhering to and efficiently wrapping DWCNTs.

## 1.	Introduction

After more than two decades of research and improvements in production processes, manufactured carbon nanotubes (CNTs) have found many applications in various fields. CNTs are already used in electronics, semiconductors, chemicals, polymers, batteries, capacitors, energy, medical, composites, aerospace and defense [1,2]. They are generally grouped into two classes: single-walled carbon nanotubes (SWCNTs) and multi-walled carbon nanotubes (MWCNTs). Among the latter, double-wall carbon nanotubes (DWCNTs) are composed of only two walls, which confer to them intermediate properties [3]. Although their production remains lower than that of MWCNTs, DWCNTs present great interest to high-tech industries that supply nanoprobes or develop composite reinforcements, energy storage media, displays, touch screens, and other electronic devices [4]. They are also of particular interest for biomedical applications [5,6]. Considering their increased uses, sooner or later CNTs will be present in substantial concentrations in the environment [7] and especially in aquatics ecosystems, which are known to concentrate many contaminants. CNTs are presumed to be non-degradable in aqueous environments [8,9] or only slightly in the presence of specific bacterial species and after long term exposure [10]. Thus, CNTs, similar to other carbonaceous nanomaterial such as fullerenes, graphene and diamonds, might remain for prolonged periods of time and strongly accumulate in aquatic media. This makes CNTs particular interesting in the study of the effects of nanostructures on organisms. However, due to the strong physical interactions of CNTs with organisms, their interference with assays or labeling, and their strong light absorption, it is difficult to assess the effect of CNTs or to identify involved mechanisms using standard toxicological assays [11,12]. Although not properly a toxic effect, the shading of photosynthetic organisms that CNTs can cause at high concentrations can also increase the globally observed inhibition of growth, especially in the case of strong adherence to organisms [13–15]. The dispersion of organic compounds such as organic matter also alters the aggregation behavior of nanoparticles in surface water and potentially their interaction with organisms [16]. An underestimation of CNTs properties and dispersion can lead to the misestimating of real toxic effects. Several recent studies point in that direction, highlighting an increased or mitigated effect of CNTs when dispersed by organic compounds such as natural organic matter (NOM) [15,17–19]. This emphasizes the importance of testing the effects of nanoparticles in environmentally relevant conditions.

Low depth aquatic environments are colonized by many benthic microorganisms that form biofilms. At the base of aquatic food chains, these organisms play a key role for many primary consumers. Numerous benthic aquatic microorganisms produce extracellular polymeric substances (EPS). These EPS are mainly composed of carbohydrates and proteins and have different roles in the environment. They are primarily used by benthic microorganisms for their aggregation and grip to substrates. This feature is known to play an important role for sediment aggregation in natural environments driven by EPS production [20,21]. The mesh formed by these EPS also allows for the retention of exo-enzymes or cellular metabolites and nutrient sequestration from the aquatic environment [24]. They may be partially recycled by organisms using it as a nutrient storage area [25]. Finally, they provide protection against different biocides [22,23], and against nanoparticles or ions that they release [26,27]. Among benthic photosynthetic microorganisms, diatoms often represent the main component of photo-autotrophic biofilms and are ubiquitous in low depth aquatic environments. This makes them responsible for more than 25% of the worldwide primary production [28]. Moreover, diatoms possess a silicified cell wall called a frustule, which confers protection against environmental dangers such as abrasion [29]. The frustule of some species also presents nano-metric pores which can partially or completely prevent the internalization of nanoparticles [27,30]. These features make them of particular interest for toxicity tests and understanding toxicity mechanisms [31].

In a previous study [27] we highlighted the strong interaction between multi-walled carbon nanotubes (MWCNTs) and the extracellular polymeric substances (EPS) produced by the benthic diatoms *Nitzschia palea* (Kützing) W.Smith (*N. palea*). It was hypothesized that EPS conferred an efficient protection against MWCNTs to benthic diatoms and that an energetic trade-off could be made by *N. palea* by switching energetic allocation from growth to protection *via* EPS production. This could explain the growth inhibition often measured only at early stages of exposure [14,27]. In this study, the toxicity of DWCNTs dispersed by an environmentally relevant amount of NOM (as it commonly happens in rivers and lakes) on the common freshwater diatom *N. palea* was assessed, focusing on growth inhibition, viability and the photochemical quantum yield of photosystem II. This work was also interested in how the presence of DWCNTs can affect EPS production, focusing on the secretion of proteins and carbohydrates and using both colorimetric assay and size exclusion chromatography. Finally, the nature of the interaction between DWCNTs and EPS were specified using a sequential extraction protocol enabling the distinct disruption of weak bounds, hydrophobic bonds, and ionic bridges.

## 2.	Experimental methods

### 2.1.	*Diatoms strain and cultures*

The axenic benthic diatom *N. palea* (CPCC-160; *N. palea*) was purchased from the Canadian phycological culture center (University of Waterloo, Waterloo, ON, Canada). Cultures were grown in CHU No. 10 basic medium (CHU10) (6.4 < pH < 6.6) (http://uwaterloo.ca/canadian-phycologicalculture-centre/cultures/culture-media/chu-10). All bioassays were performed in a growth room at $20 \pm 1\,^{\circ}$C on a rotary shaker at 90 rpm under a light/dark regime of 16 h/8 h provided by high pressure sodium lamps (VIALOX® NAV® (SON) SUPER 4Y®, 600 W, OSRAM GmbH) with an luminous intensity of 1300 cd. The media was always renewed 72 h before the experiments and prior to preparing the inoculum. All manipulations during

the experiments were carried out under a class II microbiological safety cabinet (Faster BHA 36, Faster s.r.l, Cornaredo (MI) Italy).

2.2. Natural organic matter and DWCNT suspensions

Suwannee River natural organic matter (NOM; Cat. No. 1R101N) was purchased from the International Humic Substances Society (IHSS, St. Paul, MN, USA). Prior the beginning of the experiments, NOM was hydrated with CHU10 for 1 h before being filtered (0.1-μm; Minisart high flow polyethersulfone membrane; SARTORIUS-STEDIM biotech).

DWCNTs were synthesised at the Inter-University Center for Research and Materials Engineering (Institut Carnot CIRIMAT, Toulouse, France) by CCVD synthesis. The CNTs fraction contained DWCNTs (∼80%), SWCNTs (∼15%), and MWCNTs (∼5%) [3]. Their length was between 1 and >100 μm with an outer diameter of between 1 and 3 nm (determined by transmission electron microscopy) for a surface area of 980 m^2/g (determined using Brunauer, Emmett and Teller theory). The samples exhibited a Raman spectroscopy Id/Ig ratio of 0.24 ± 0.05 in (Fig. 1a; ± indicates the standard deviation; Horiba Jobin Yvon LabRAM HR800 Raman micro-spectrometer at 633 nm, red laser excitation, He/Ne).

The dry sample was composed (mass fraction) of carbon (92.13 ± 0.46%) cobalt (3 ± 0.15%), molybdenum (0.9 ± 0.04%) and iron (0.04 ± 0.004%) [32].

Four DWCNT suspensions (0.167, 1.67, 16.7, 83.5 mg L^{-1}) were made using CHU10 from a stock suspension which was first sonicated for 1 h (BRANSON digital sonifier S-250D; 200 W; amplitude: 35% 5 s/2 s). NOM (16.7 mg L^{-1}) followed by addition of the DWCNT suspensions, which were then sonicated again for 20 min. These solutions were diluted in culture or CHU10 to obtain exposure concentrations of 0.1, 1, 10 and 50 mg L^{-1} of DWCNTs and 10 mg L^{-1} of NOM. At this environmentally relevant concentration [33], NOM strongly coated both the individual and bundled DWCNTs (Fig. 1b and c). As assessed by optical density, the suspensions appeared stable for 0.1–1 mg L^{-1} while sedimentation occurred quickly from 10 mg L^{-1} (<1 h). Sonication did not cause disruption of the DWCNTs (determined by transmission electronic microscopy and Raman analyses; Fig. 1a and c). The detectable CHU10-soluble metallic residues released by DWCNTs 50 mg after 48 h were cobalt (33.56 ± 0.18 μg L^{-1}), molybdenum (222.78 ± 1.85 μg L^{-1}) and iron (176.41 ± 43.3 μg L^{-1}) (inductively coupled plasma mass spectrometry; ICP-MS; Agilent-7500ce, Agilent Technologies, Palo, CA).

2.3. Growth and toxicity tests

2.3.1. Exposure strategy
The toxicity of DWCNTs was assessed by determining the effects on growth, photochemical quantum yield of photosystem II, and viability. These tests were carried using the same device as used in a previous study [27]. Briefly, two stacked 12-well plates allowed for the assessment of the total exposure effect, providing an estimation of shading using DWCNT suspensions as external filters. Lower plates were inoculated with 1 mL per well of N. palea suspensions (2.5·10^5 cells/mL) and were grown for 24 h in culture conditions but without
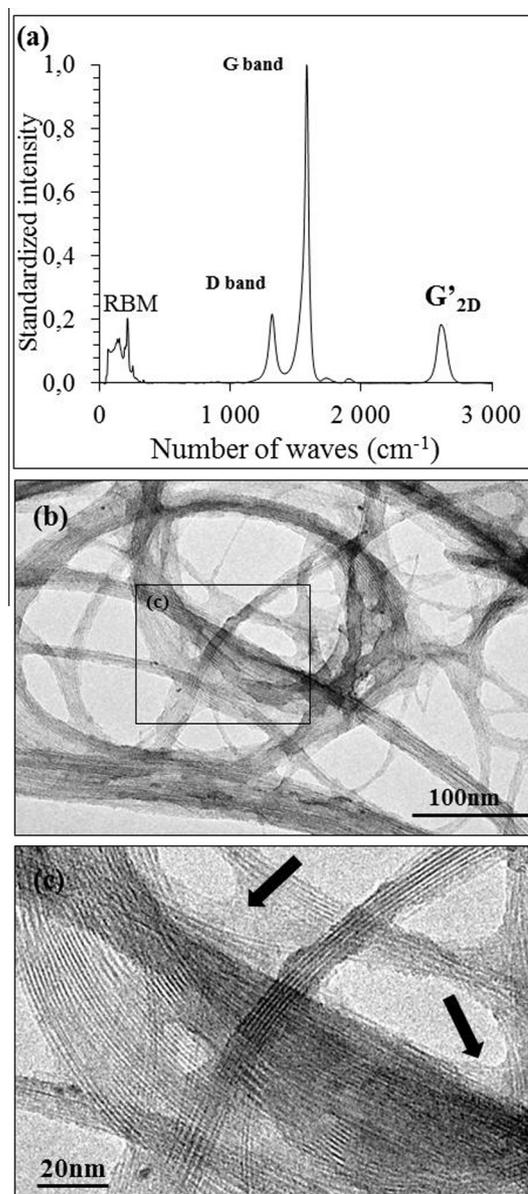
Fig. 1 – (a) Raman spectra of double-walled carbon nanotubes (DWCNTs). In the upper right, the D-band is normalized with respect to the intensity of the G-band intensity of the same spectra. (b) General transmission electron microscopy view of DWCNTs after drying the DWCNT suspension (10 mg L^{-1}) dispersed with natural organic matter (NOM; 10 mg L^{-1}). (c) A magnified view of (b) highlighting the affinity of NOM for DWCNTs. Arrows indicate the presence of NOM. Image of DWNTC without NOM is given in Supplementary material 1.

shaking. This step allowed the diatoms to adhere, recover their growth and reach the exponential phase. Then, the bottom wells were filled with DWCNT suspensions (1.5 mL), obtaining final DWCNT concentrations of 0.1, 1, 10 and 50 mg L^{-1} or with CHU10 + NOM for controls and shading tests. Upper plates were prepared following the same protocol but the wells were filled using CHU10 + NOM for exposure

tests and with DWCNT suspensions for shading tests, which used external light filters. The rest of the wells were filled with CHU10 to obtain the same final volume in each well. One plate per condition was prepared for the control and for exposure to each concentration of DWCNTs.

2.3.2. Growth tests

Shading caused by DWCNTs was assessed by measuring photosynthetically active radiation (PAR; Li-250A light meter equipped with Li-COR Quantum sensor; Li-COR Biosciences, San Diego, CA) under the upper plates of the shaded plates at the beginning of the test. At 48 and 144 h, 3 wells per plates were scraped, sampled and fixed in formaldehyde 3.6%. The algal concentrations were determined using a Malassez cell counter performing two counts per well. Significant differences between conditions were determined by one way analysis of variance (ANOVA) followed by Tukey HSD post hoc tests using the statistical open source software "R" (SSR; R Development Core team 2012, Bio-RAD, Charlottesville, VA). At 48 h of exposure during exponential growth of control cultures, the effective concentrations of 50% (EC_{50}) were determined with the Excel®macro REGTOX 7.0.3 (copyright© 2001, Eric Vindimian) using the Hill model. The 95% confidence intervals for the EC_{50} values were calculated by bootstrap simulations ($n = 500$). The correlation between PAR and growth inhibition was assessed using Pearson's correlation test.

2.3.3. Viability tests

The lethal effect of CNTs was assessed under fluorescent microscopy using Sytox green®. This dye only penetrates injured or dead cells and labels their nuclei while it is excluded from entering healthy cells. After 48 h of exposure, a part of the living samples from the growth tests were incubated for 10 min in Sytox green (120 nM in dimethylsulfoxide) and then observed using a fluorescence microscope (BX-41, Olympus, Center Valley, PA) equipped with an Hg lamp (U-LH100HG, Olympus, Center Valley, PA) using a 470–490 nm/520 nm excitation/emission filter and a 500 nm dichromatic filter (U-MNB2, Olympus, Center Valley, PA). The concentration of dye was calibrated to allow for efficient labeling without significant interference caused by DWCNTs [34]. Significant differences were assessed using non-parametric Kruskal–Wallis analysis of variance.

2.3.4. Effect on photosynthesis

The effects of DWCNTs on photosynthesis was evaluated after 48 h of exposure by pulse amplitude modulation (PAM) using a Phyto-PAM (Heinz Waltz GmbH, Effeltich, Germany) to establish the effective quantum yield of photochemical energy conversion in photosystem II (PSII). This method determines electron transfer efficiency along the photosynthetic chain by establishing the ratio of emitted photons to chlorophyll-absorbed photons after an illumination pulse. The higher the value for PSII, the more efficient the electron transfer is and the less it is impacted by a pollutant. Measurements were done after 30 min in the dark. Significant differences between conditions were determined by Kruskal–Wallis analysis of variance.

2.4. Extracellular polymeric substances assays

2.4.1. Culture and extraction protocols

This experiment was conducted in plastic flasks (Corning® cell culture flasks Ref. 431080, surface area 175 cm², Corning Tewksbury MA, USA). Flasks were first inoculated with 100 mL of N. palea suspension (2.5 cell mL^{-1}) and grown for 24 h (at $20 \pm 1\,°C$) without shaking. Then, DWCNT suspensions (150 mL) were added to cultures at concentrations of 0, 1.67, 16.7 mg L^{-1} to reach final concentrations in the flask of 0 mg L^{-1} (control), 1 and 10 mg L^{-1}, respectively. After 8 days of exposure, the samples reached the stationary phase and similar algal concentrations in all assessed conditions. The biofilms were scraped and vigorously shaken and centrifuged. EPS were then extracted following the multi-methods sequential protocol previously described by Ras et al. [35], but without sonication to prevent diatom lysis. One extraction sequence involving three steps was applied in sequence with intermediate centrifugations (3200g; 10 min) to collect the supernatants, which contained the solubilized EPS. Pellets were first incubated for 1 h at 20 °C in 20 mL of phosphate buffered saline (PBS) pH 7.4. The recovered pellet was then incubated in 4 mL PBS containing Tween® 20 (0.25%) for 1 h at 20 °C. The third extraction step was performed using 4 mL of the cationic chelator EDTA (1% EDTA in Tris–HCl 0.3 mol L^{-1}, pH 8.5) for 1 h at 20 °C. Supernatants were stocked at 4 °C (<24 h) before analyses. The remaining pellets (EPS residues + cells + DWCNTs) were diluted in 20 mL of PBS before quantification of the residual fraction (cellular content + EPS residues).

Each extraction step was done under gentle agitation using a rotary disc shaker. This separation method allowed for the isolation of EPS that was linked to DWCNTs through (i) weak bonds ($H_2O_{extract} + PBS_{extract}$), (ii) hydrophobic bonds ($TWEEN_{extract}$) and (iii) ionic bridges ($EDTA_{extract}$). Samples of pellets were obtained at the end of the extraction before quantification of the residual fraction, and the efficiency of extraction was controlled by light microscopy using Alcian blue as an EPS labeler [25]. Cellular integrity was controlled at the same time as described in the viability tests section.

2.4.2. Proteins and carbohydrates quantification

Carbohydrate measurements were performed for each extract by the anthrone method [34,36]. 200 µL of anthrone reagent (2% in 96% sulfuric acid) was added to 100 µL of each extracted sample in 96-well plates. The mixtures were then incubated at 60 °C for 60 min and then cooled at room temperature for 10 min before light absorbance was measured at 620 nm using a microplate reader (FLUOstar, BGM Labtech, Orthenberg, Germany). Glucose was used as standard.

Proteins were measured using the bicinchoninic acid (BCA) reagent (Sigma–Aldrich). A 25 µL assay sample was added to 200 µL of BCA reagent in a microplate. When samples contained EDTA, a 20 µL assay sample was added to 1 mL of BCA reagent to avoid underestimation of the protein content due to chelation between EDTA and the Cu^{2+} contained in the BCA reagent. Bovine serum albumin (BSA) was used as a standard [37]. Absorbance was measured at 560 nm with a microplate reader (FLUOstar, BMG Labtech, Orthenberg, Germany).

The background signals of the DWCNT suspensions were always removed. No significant interference of the DWCNTs or of NOM was observed on reagents (anthrone and BCA) at the tested concentrations (data not shown). Significant differences between conditions were determined using SSR by analyses of variance (ANOVA) following by Tukey HSD post hoc when significance was observed. Correlations between DWCNT concentrations and measured protein and carbohydrate contents were determined by Pearson correlation tests when significant differences were observed.

2.4.3. *Extracellular polymeric substances size distribution*

The size of EPS was determined using high performance liquid chromatography (HPLC; AKTA Purifier, GE Healthcare, Fairfield, CT, USA) equipped with a 500 μL injection loop. Size exclusion chromatography was performed using a 24 mL column containing 13 μm of a spherical composite matrix of cross-linked agarose and dextran with a separation range of 10,000–600,000 Da (Superdex 200 10/300 GL column; AKTA GE Healthcare, Fairfield, CT, USA). Absorbance was measured at 210 nm (non-specific absorbance) and 280 nm (absorbance specific to cyclic amino acids). The values of the extracting solutions (PBS, TWEEN® 0.25% in PBS and EDTA, 1% in Tris–HCl) were removed from the various extract signals. The sizes of the extracted molecules were calculated from a calibration curve obtained using a mix of different proteins (dextran blue: 2106 kDa, thyroglobulin: 669 kDa, ferritin: 440 kDa, conalbumin: 75 kDa, ovalbumin: 44 kDa, carbon anhydrase: 29 kDa, ribonuclease: 13.7 kDa, aprotinin: 6.5 kDa) according to the following equation: $y = 4 \cdot 10^{8}, x^{-5.876}; R^{2} = 0.996$, where y is in Da and x is in mL (peak elution volume). Due to the risk of contamination by DWCNTs, the first peak corresponding to the large-sized molecules ($>2 \cdot 10^{6}$ Da) was not considered.

2.5. *Scanning electron microscopy*

Interactions between DWCNTs and the biofilm of *N. palea* were investigated by field effect gun scanning electron microscopy (SEM) focusing on the adherence of DWCNTs to the biofilm.

N. palea was grown in the same devices as those used for toxicity tests but with glass coverslips placed at the depth of well. After 48 h of exposure to DWCNTs$_{10mg}$, the samples were fixed (Sigma–Aldrich, France) as described in [27]. Briefly, this process consisted of a 24 h fixation in a solution of 0.1% Alcian blue (No. CAS: 33864-99-2), acetic acid (0.5 M), paraformaldehyde (2%) and glutaraldehyde (2%) buffered using sodium cacodylate (0.15 M), followed by a subsequent 2 h post-fixation in a solution of potassium ferro-cyanide (1.5%) and OsO_4 (1%) buffered by cacodylate. After rinsing, the samples were dehydrated in an ascending ethanol gradient before being dried under N_2 flux at room temperature. They were finally placed on SEM mounts and platinum-coated before observation (JEOL JSM-6700F, 3 kV, Tokyo, Japan).

3.   Results

3.1.   *Toxicity tests*

The results of the growth inhibition test are summarized in Table 1.

48 h of direct exposure to DWCNTs led to significant inhibition of growth at concentrations ranging from DWCNTs$_{1mg}$ (~30%) to DWCNTs$_{50mg}$ (~85%). The 48 h EC$_{50}$ was 7.5 mg L^{-1} (at a 95% confidence interval of 3.9/13.3). Moreover, the inhibition was not significantly correlated with PAR (cor = 0.55; $p = 0.06$). The shading effect on growth was only significant at concentrations ranging from DWCNTs$_{10mg}$ (~20%) to DWCNTs$_{50mg}$ (~40%). It corresponds to the two DWCNT concentrations where PAR significantly decreased relative to the control. Furthermore, inhibition in the shading tests was positively correlated with a decrease in PAR (cor = 0.86; $p < 0.001$). This was not the case for the direct exposure tests (cor = 0.54; $p = 0.07$). After 144 h, the inhibition of growth was only significant for cultures directly exposed to DWCNTs$_{50mg}$ (~30%) indicating only a partial recovery of growth while all other conditions exhibited a complete growth recovery over the considered period. DWCNTs$_{50mg}$ did not induce mortality (6.63 ± 2.17%; ± indicates the standard deviation) compared to control (7.37 ± 1.1%). The PSII quantum yield was also

Table 1 – Summarized results of the toxicity tests. The first four lines represent the inhibition of growth (%) under direct exposure or shading. 48 h-EC$_{50}$ is the exposure concentration of DWCNTs that caused 50% inhibition of growth after 48 h of direct exposure (during the exponential phase). 48 h-PSII are the values of the photochemical quantum yield of photosystem II after 48 h of direct exposure to DWCNTs. Finally, the PAR values represent the photosynthetic active radiation received by diatoms after passing through DWCNT suspensions. Gray values indicate the standard deviation. For any considered line, two groups without any letters in common are significantly different ($p < 0.05$).

	Control			DWCNT$_{0.1mg}$			DWCNT$_{1mg}$			DWCNT$_{10mg}$			DWCNT$_{50mg}$		
48 h exposure (%)	0		a	13.7	8	a	29.2	1	b	46.4	3	c	84.1	10	d
48 h shading (%)	0		a	3.9	5	a	−1.0	0.3	a	21.5	7	b	40.6	17	b
144 h exposure (%)	0		a	−4.0	4	a	2.0	5	a	7.0	2	a	27.4	2	b
144 h shading (%)	0		a	1.0	1	a	3.3	4	a	-3.5	3	a	−3.2	3	a
48 h-EC$_{50}$ (mg L^{-1})	7.5 (95% confidence interval: 3.9/13.3)														
PSII quantum yield	0.63	0.01	a	0.66	0.01	a	0.66	0.02	a	0.66	0.01	a	0.64	0.01	a
PAR (μmoles s^{-1} m^{-2} μA)	23.9	1.5	a	21.9	1.4	a	23.7	1.3	a	17.3	1.3	b	14.9	3.4	b

unaffected by the presence of DWCNTs regardless of the concentration and always exhibited value of 0.65 ± 0.01.

## 3.2. Quantification of carbohydrate and protein contents of extracted EPS

After extraction with the multi-methods protocol, carbohydrates and proteins composing the total extracted EPS were quantified using colorimetric assays (Fig. 2).

Proteins were significantly higher for samples exposed to DWCNTs (control: 31.23 ± 3.84 mg L^{-1}; DWCNTs$_{1mg}$: 49.95 ± 6.86 mg L^{-1} and DWCNTs$_{10mg}$: 49.06 ± 6.49 mg L^{-1}) and no significant difference was revealed between the two tested concentrations (± indicates the standard deviation). On the other hand, the carbohydrate assays showed no difference regardless of the DWCNT concentration tested (control: 13.72 ± 4.13 mg L^{-1}, DWCNTs$_{1mg}$: 12.6 ± 3.33 mg L^{-1} and DWCNTs$_{10mg}$: 15.46 ± 3.3 mg L^{-1}). Thus, in the absence of DWCNTs, the total amount of extracted EPS was 44.95 ± 5.3 mg L^{-1} and corresponded to a proteins/carbohydrates ratio of 2.27. After exposure to DWCNTs$_{1mg}$ and DWCNTs$_{10mg}$, the EPS amounts were 62.56 ± 5.26 and 65.14 ± 5.02 mg L^{-1} and corresponded to increased proteins/carbohydrates ratios of 3.96 and 3.05, respectively.

3.3. Characterization of extracted EPS by size exclusion HPLC

Global (210 nm) and protein (280 nm) profiles of the different EPS fractions (PBS$_{extract}$, TWEEN$_{extract}$, and EDTA$_{extract}$) extracted from the control, DWCNT$_{1mg}$ and DWCNT$_{10mg}$ cultures were analyzed by size exclusion HPLC (Fig. 3).

Each fraction exhibited singular profiles and exposure to DWCNTs with affected peak amplitudes rather than molecular weight distributions. Indeed, PBS$_{extract}$ profiles at 210 nm
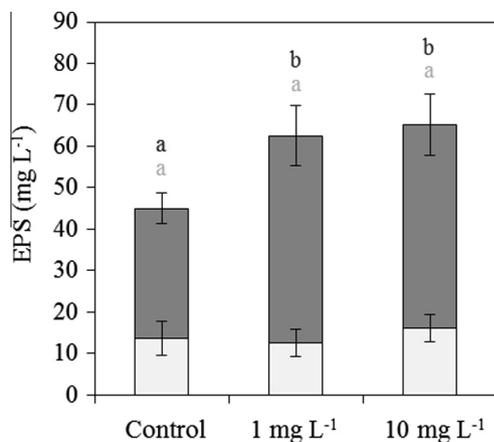

Fig. 2 – Results of the assays measuring total amounts of carbohydrates (anthrone test) and protein-like polymers (BCA test) depending on the DWCNT concentration. Dark bars are proteins (in an equivalent amount of bovine serum albumin) and bright are carbohydrates (in an equivalent amount of glucose). Two groups without any letter in common are significantly different ($p < 0.05$). The details of each fraction are given in Fig. 4.

(Fig. 3a) showed three main peaks in the control and treated cultures (elution volume: Ev = 19.7 mL $\sim$ 10 kDa, 22.05 mL $\sim$ 5 kDa, 24.6 mL $\sim$ 3 kDa). Meanwhile, the protein profile of the PBS$_{extract}$ at 280 nm (Fig. 3d) showed one peak (Ev = 19.7 mL) with a similar area for the three analyzed PBS extracts. The TWEEN$_{extract}$ profiles at 210 nm (Fig. 3b) showed six major peaks occupying the same positions on the chromatographs for different conditions (Ev = 11.2 mL $\sim$ 273.4 kDa, 12.1 mL $\sim$ 174 kDa, 16.1 mL $\sim$ 32 kDa, 19.7 mL $\sim$ 10 kDa, 22.7 mL $\sim$ 4 kDa, 2 4.6 mL $\sim$ 3 kDa) but with different amplitudes. This was especially the case for DWCNTs$_{10mg}$, in which the peaks that eluted between 16 and 23 mL were strongly increased. Among these, only two peaks were present at 280 nm (12.1 mL $\sim$ 174 kDa and 19.7 mL $\sim$ 10 kDa; Fig. 3e), suggesting that they were mainly composed of protein-like polymers (proteins or glycoproteins, PLPs) with either high or low molecular weights. Finally, the EDTA$_{extract}$ profiles showed four distinct peaks at 210 nm (Ev = 13.5 mL $\sim$ 91 kDa, 15.6 mL $\sim$ 39 kDa, 25.7 mL $\sim$ 1 kDa; Fig. 3c). At 280 nm, only two peaks (15.6 mL $\sim$ 39 kDa; 19.7 mL $\sim$ 10 kDa; Fig. 3f) were detected with higher amplitudes in the DWCNTs$_{10mg}$ extract compared to the control and DWCNTs$_{1mg}$ chromatographs. A Tris–EDTA signal between $\sim$20 and 24 mL was over the detection limit and was not considered.

3.4. Chemical interaction between EPS and DWCNT

A multi-method extraction processed allowed for the fractionation of EPS according to chemical and physical interactions within the biofilm. The collected EPS fractions can be divided according to their interactions with DWCNTs: (i) weakly linked (H$_2$O$_{extract}$ + PBS$_{extract}$), (ii) linked by hydrophobic bonds (TWEEN$_{extract}$), and (iii) linked by ionic bridges (EDTA$_{extract}$). Fig. 4 shows the quantitative distribution of carbohydrates and proteins in the recovered fractions after incubation in the absence (control) or in the presence of DWCNTs$_{1mg}$ and DWCNTs$_{10mg}$.

The weakly bounded EPS fraction (Fig. 4a) showed no significant difference in either the carbohydrate or protein secretion ($p > 0.05$) between the three tested conditions. The TWEEN$_{extract}$ contained a significantly higher concentration of carbohydrates in DWCNT$_{10mg}$ ($p < 0.01$) than either the control or DWCNTs$_{1mg}$. (Fig. 4b). Moreover, the concentrations of carbohydrates and DWCNTs were positively correlated (cor = 0.88; $p = 0.001$). The protein contents of TWEEN$_{extract}$ were significantly different under all conditions and were also strongly correlated (cor = 0.92; $p < 0.001$) with the DWCNT concentration. EDTA$_{extract}$ exhibited no difference or correlation regardless of the concentration of DWCNTs (Fig. 4c). The residual fractions (EPS residues + cellular content + DWCNTs) were also assessed. Neither carbohydrates (control: 1.07 ± 0.11 pg cell^{-1}, DWCNTs$_{1mg}$: 1.20 ± 0.16 pg cell^{-1}, DWCNTs$_{10mg}$: 1.32 ± 0.21 pg cell^{-1}) nor proteins (control: 6.13 ± 0.1 pg cell^{-1}, DWCNTs$_{1mg}$: 6.51 ± 0.91 pg cell^{-1}, DWCNTs$_{10mg}$: 5.99 ± 2.05 pg cell^{-1}) were significantly different between the different conditions. In addition, Alcian blue staining did not reveal any remaining EPS at the end of the extraction. There was also no difference in mortality between the three conditions tested (results not shown).
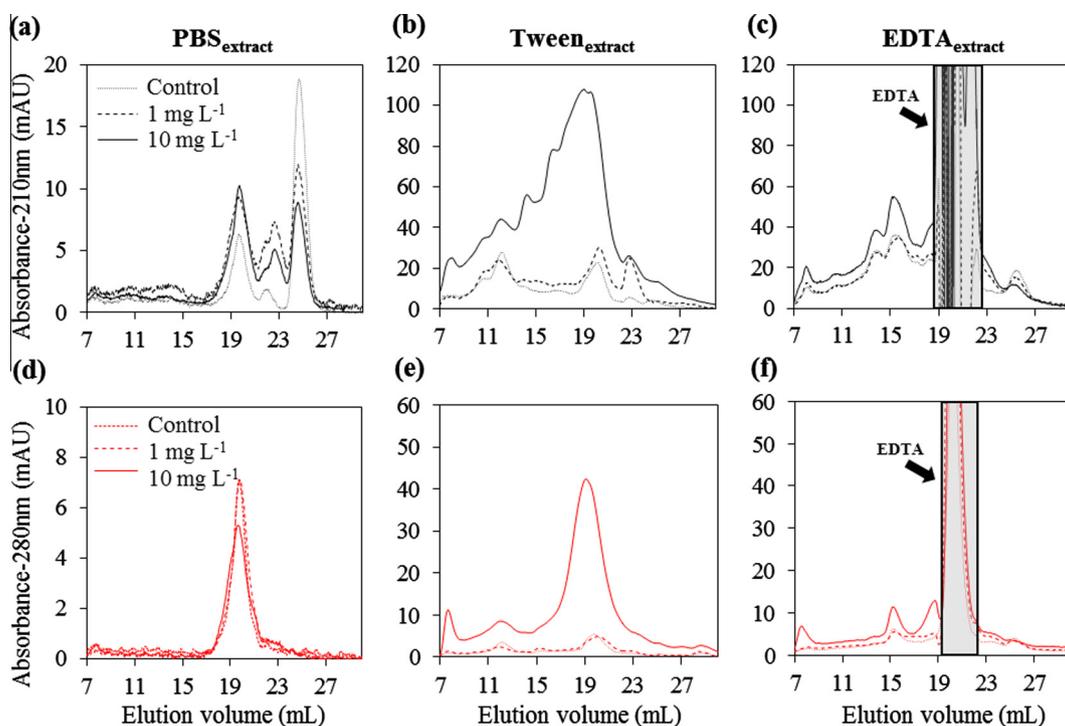
Fig. 3 – Size exclusion high precision liquid chromatography (HPLC) profiles of EPS extracted with (a) and (d) phosphate buffer saline (PBS$_{extract}$); (b) and (e) TWEEN 20 (TWEEN$_{extract}$); and, (c) and (f) Tris–EDTA (EDTA$_{extract}$). (a)–(c) Are nonspecific absorbance profiles at 210 nm showing both carbohydrates and protein-like polymers, while (d)–(f) are absorbance profiles at 280 nm showing only protein-like polymers. Samples from the TWEEN$_{extracts}$ and EDTA$_{extracts}$ were 5 times more concentrated than those of the PBS$_{extracts}$ (cf. Experimental Methods). Note that in (c) and (f), the peak starting at 19.6 corresponds to EDTA and not an extracted molecule. The first peak (∼8 mL) from each condition corresponds to large molecules or the assembly of molecules (or, potentially, remaining DWCNTs) that were excluded from the column.

3.5. Physical interaction between DWCNTs and biofilm

Fixation of EPS followed by SEM was implemented to visualize the interaction between the biofilm and DWCNTs (Fig. 5).
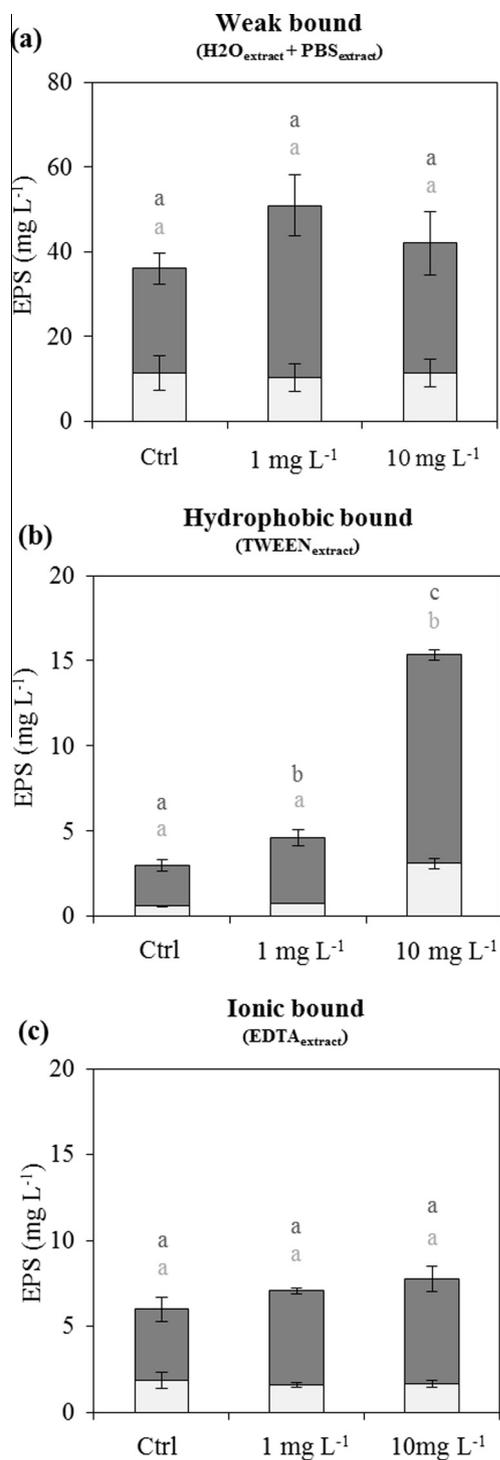
Fig. 5a shows a picture from the control culture revealing the thin EPS network produced by *N. palea*. Fig. 5b shows the biofilm exposed to DWCNTs$_{10mg}$, emphasizing a strong disruption of the EPS network in the presence of DWCNTs. However, no interaction between the frustule and DWCNTs was shown. A higher magnification (Fig. 5c) revealed DWCNT bundles inside the disrupted EPS. This picture also shows the strong affinity of EPS for DWCNTs, which was mostly coated by EPS.

4. Discussion

4.1. Toxicity of DWCNT

In this study, both the effects of direct exposure to DWCNTs and shading using DWCNTs as an external filter on *N. palea* growth were evaluated. DWCNTs toxicity was assessed using assays measuring the decreases in viability and PSII quantum yield. The results summarized in Table 1 are close to those previously obtained for the effect of MWCNTs on *N. palea* using identical experimental conditions [27]. After 48 h, externally shaded cultures showed a growth inhibition only from DWCNTs$_{10mg}$ (∼22%) to DWCNTs$_{50mg}$ (∼41%), which is well-correlated with PAR decreases (DWCNTs$_{10mg}$ ∼ 27%; DWCNTs$_{50mg}$ ∼ 37%; cor = 0.86; $p < 0.001$). Over the same time period, direct exposure to 1 mg L^{-1} (∼30%) to 50 mg L^{-1} (∼84%) of DWCNTs resulted in a significant and dose-dependent growth inhibition. Even though this result was not significantly correlated with a PAR decrease (cor = 0.54; $p = 0.07$), a shading effect resulting from the agglomeration of DWCNTs to algae cannot be excluded at low concentrations and might partially act in the observed growth inhibition [38,39]. In contrast, after 6 days (144 h) of direct exposure, cultures entirely recovered their growth rate in the range of DWCNTs 0.1 mg to DWCNTs 10 mg. This recovery was partial with DWCNTs 50 mg (∼30%). This temporary growth inhibition of algae has been frequently observed in the presence of CNTs and is generally explained by the agglomeration of CNTs facilitated by their specific affinity and the molecules produced by exposed organisms, which both decrease the interaction of CNTs with surfaces over time [14,40]. Finally, shaded cultures completely caught up their growth and presented a similar concentration of diatoms to the controls in stationary phase. Thus, in our experimental conditions, the PAR decreases caused by the highest concentrations of DWCNTs only limited cell division. This could also partially explain the growth recovery in the direct exposure tests. The presence of metallic impurities is occasionally put forward to explain the observed toxicity during exposure to CNTs [41,42]. In this study, concentrations of metal ions in

(a) Weak bound
(H2O$_{extract}$ + PBS$_{extract}$)

(b) Hydrophobic bound
(TWEEN$_{extract}$)

(c) Ionic bound
(EDTA$_{extract}$)

Fig. 4 – Results from the colorimetric assays of each extracted fraction ranked by bonding properties. (a) Weak or mechanical bonds between DWCNTs and organisms (H$_2$O$_{extract}$ + PBS$_{extract}$). (b) Linked by hydrophobic bound (TWEEN$_{extract}$). (c) Linked by ionic bridges (EDTA$_{extract}$). Error bars indicate the standard deviation. For each graph, two groups without any letter in common are significantly different ($p < 0.05$). Global concentrations of extracted EPS (obtained from the addition of these different fractions) are given in Fig. 2.
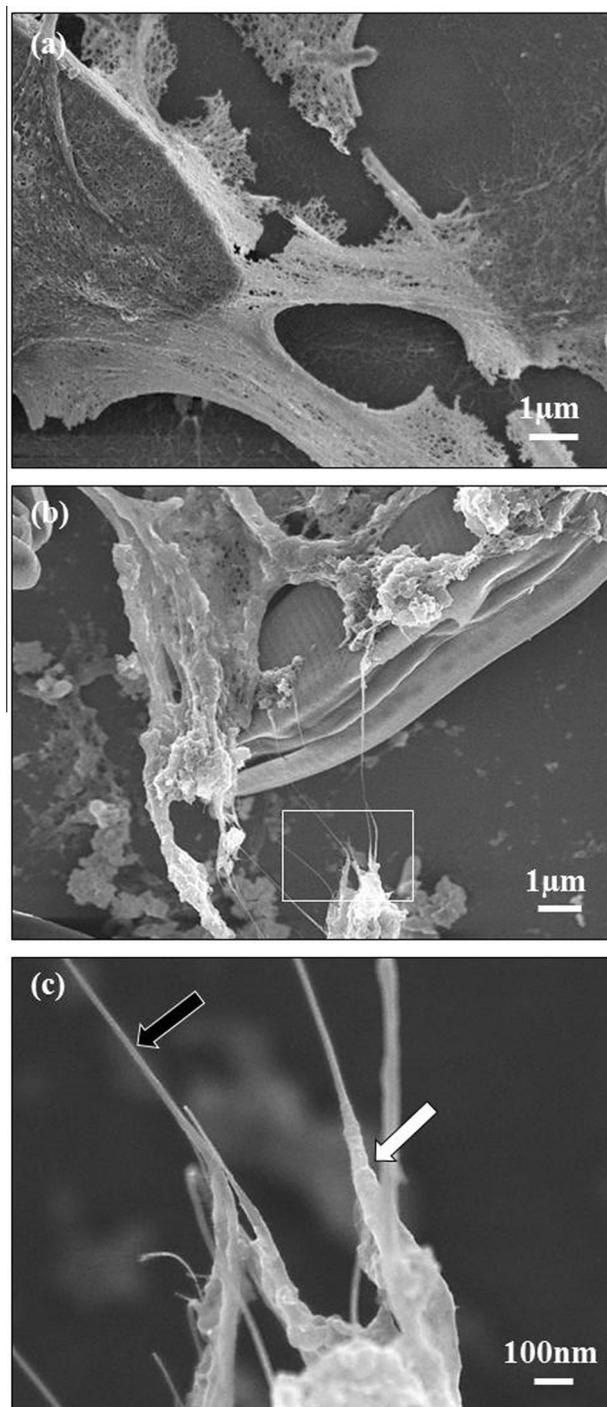
Fig. 5 – Scanning electron microscopy observations of (a) the control biofilm and (b) the biofilm exposed to 10 mg L^{-1} of double-walled carbon nanotubes (DWCNTs). (c) A magnified view of (b) highlighting the thin interactions between EPS and DWCNTs and the disrupted aspects of EPS in the presence of DWCNTs. The black arrow indicates a DWCNT bundle. The white arrow shows EPS wrapping around a bundle of DWCNTs.

solution from the DWCNT suspensions were ten times lower for cobalt ($\sim$34 μg L^{-1}) and forty times lower for molybdenum ($\sim$222 μg L^{-1}) than those causing effects on various unicellular

green algae and diatoms [43–45]. The iron content of the $DWCNT_{50mg}$ solution was only increased by ∼7% compared to the amount inherent to the CHU10 concentration (2.5 mg L^{-1}). Moreover, metallic particles were mainly embedded inside carbon shells which avoid direct interaction with organisms. Finally, no increase in mortality or decrease in PSII quantum yield was observed (Table 1). These results highlight a delaying effect of DWCNTs on the growth of *N. palea* rather than a toxic effect.

4.2. DWCNT effect on EPS production and possible involvement in growth delay

The effects of DWCNTs on EPS production by *N. palea* was assessed using anthrone (carbohydrates) and BCA (proteins) colorimetric assays performed on extracted EPS fractions. Unlike what is generally reported in the literature but has already been highlighted by some authors [46,47], this study found that protein was actually the primary part of extracted EPS. Thus, this fraction of EPS should always be considered in future studies dealing with the EPS of diatoms.

In this study, the data revealed a higher EPS production in cultures exposed to DWCNTs (Fig. 2), indicating that the amount of EPS produced by microorganisms can be driven by environmental conditions [35,48,49]. EPS allows for the adherence of benthic organisms to substrates. EPS secretions are also known to decrease water turbidity by aggregating suspended particles while allowing for the movement of diatoms to brighter areas [20,50,51]. In this work, the overproduction of EPS could therefore lead to decreased turbidity of the medium, increasing the catching efficiency of DWCNTs by the biofilm. It can also reflect the efficiency of the diatoms to move in an attempt to reach brighter areas while leaving behind the DWCNTs-adhered areas. EPS are also known to protect organisms from particulate abrasion [22,29] and against many biocides [23]. Some authors highlighted an enhanced resistance of bacteria against TiO_2 and silver nanoparticles conferred by an overproduction of EPS [52,53]. In the present study, EPS could perform the same function against the DWCNTs by covering them, reducing the possibility of direct contact between the DWCNTs and cells, as already reported by some authors [14,27,40,54] and highlighted by SEM (Fig. 5). Another interesting finding is that the overproduction of EPS was similar between $DWCNTs_{1mg}$ and $DWCNTs_{10mg}$. On the one hand, it cannot be excluded that the decrease in PAR from $DWCNTs_{10mg}$ could have limited the photosynthetic activity and thus EPS production [55,56]. On the other hand, this result suggests that *N. palea* responded in a massive way from exposure to $DWCNTs_{1mg}$ to both limit its contact with particles and to improve the brightness of the water column [55]. Despite the energetic cost, this response may constitute a considerable benefit in this case. From an adaptive perspective, the overproduction of EPS can provide maximum protection from weaker doses of CNTs. Some diatoms are also known to use extracellular carbohydrates as an energy reserve, and can use a portion of the carbohydrates produced on a daily basis to ensure the continuity of growth and cell function during the night [25,56]. However, interactions between DWCNTs and EPS might limit carbohydrate recycling during the night. The fact that the

amounts of extracted carbohydrates were similar between the three assessed conditions suggests that DWCNTs did not appreciably limit the EPS recycling.

Finally, the overproduction of EPS could explain the higher growth delay observed in the 48 h cultures directly exposed to $DWCNTs_{0.1mg}$ and $DWCNTs_{1mg}$ while neither a decrease in growth or in PAR were observed in the shaded cultures. Even if we cannot rule out the underestimation of the shading effect from the external filters, the energetic cost of EPS overproduction could at least partially explain the observed inhibition of directly exposed cells. From the growth inhibition results (Table 1) and EPS production (Fig. 2), the energy expenditure related to the overproduction of EPS seems to be responsible for ∼100% of the growth inhibition in diatoms in direct contact with $DWCNTs_{1mg}$ whereas only ∼60% of the growth inhibition in $DWCNTs_{10mg}$ is linked to EPS overproduction and ∼40% is due to shading. These estimates are consistent with other works on *Chlorella* sp. exposed to MWCNTs [40] but are different from other studies [15] in which the inhibition by shading during exposure was considered to be ∼67%. This study underlines a potential additive effect of two mechanisms that are responsible for the temporary growth inhibition of *N. palea* when directly exposed to DWCNTs: (i) the energy cost of EPS overproduction, which can cause the agglomeration of MWCNTs both to themselves and to organisms, and (ii) the shading caused by MWCNTs.

4.3. DWCNT effect on EPS distribution

Analysis of the different EPS fractions by size exclusion chromatography revealed three distinct profiles with peak amplitudes related to the concentrations of DWCNTs (Fig. 3). This result, as well as those of the EPS assays (Fig. 2), indicates that in the presence of DWCNTs, *N. palea* can increase EPS production (specifically PLPs) without strongly changing the size of molecules produced. In the $PBS_{extract}$, four separate peaks were detected at 210 nm that correspond to low molecular weight molecules with sizes ranging from 3 to 10 kDa. Among these molecules, only one (∼10 kDa) was a PLP. These molecules can correspond to fragments of proteins or glycoproteins that were easily detached from the biofilm due to previous digestion of the matrix by extracellular proteases. Six distinct fractions were eluted from the column using TWEEN as a detergent for the extraction of hydrophobic molecules. The eluted molecules exhibited a wide range of sizes ranging from 273.4 to 3 kDa. Among these, two fractions were PLPs, one contained high molecular weight proteins approximately 174 kDa, and the last contained low molecular weight proteins approximately 10 kDa. Notably, a ∼10 kDa PLP was present in large amounts in the $PBS_{extract}$, the $TWEEN_{extract}$ and the $EDTA_{extract}$ and could be the same molecule in each sample. This finding indicates that this molecule might be heavily involved in the DWCNT/EPS interaction. The EDTA extract contained four different molecules with sizes ranging from 1 to 91 kDa (Fig. 3c). The 39 kDa and the 10 kDa fractions were detected at 280 nm as PLPs. This indicates that the 10 kDa molecules might be heavily involved in the DWCNT/EPS interaction and, even if a large part remains unlinked to DWCNTs, some of them are linked to the biofilm and can be extracted after the disruption of

chemical interactions. Interestingly, a protein-like polymer with an intermediate molecular weight of 39 kDa was only found in the EDTA extract. The 39 kDa peak was, however, increased for DWCNTs[10mg], suggesting that this molecule could either bridge with divalent ions in functionalized areas of DWCNTs that contain structural imperfections or non-covalently functionalize NOM to cover CNT. As previously described by Caudan et al. [57], anionic proteins and divalent calcium were reported to be key components for the aggregation of microbial granules involved in the elimination of organic components. Due to the presence of negative carboxyl groups on the glutamic and aspartic amino acids of proteins, this mechanism may be involved in the formation and stability of many other biological matrixes, including diatom biofilms.

4.4. Interactions between DWCNTs and EPS

The adhesion of CNTs to algae has often been observed [14,15,40,58]. In this study, HPLC (Fig. 3) and carbohydrates/proteins assays (Fig. 4) for each extracted fraction as well as SEM (Fig. 5) were implemented to better understand the nature of the interactions between EPS and DWCNTs. Water-soluble and weak bonds between EPS and DWCNTs were obtained in the $H_2O_{extract}$/$PBS_{extract}$, hydrophobic bonds were obtained in the $TWEEN_{extract}$, and or bridged interactions between divalent ions were obtained in the $EDTA_{extract}$.

No significant difference was observed in the $H_2O_{extract}$/$PBS_{extract}$ after DCWNTs exposure. However, this sample constituted a majority of the produced EPS reaching ~50% and ~60% of the total EPS amount. These EPS could be involved in the mechanical action occasionally used to explain the interaction between DWCNTs and organisms [14,15] or EPS [27,54]. TWEEN 20 was used as a chemical substitute for hydrophobic bonds [59], freeing the EPS linked by hydrophobic interactions to DWCNTs. Considering the high solubility of polysaccharides, the hydrophobicity of EPS is mostly inherent to proteins [49,60]. In this study, carbohydrates and PLPs from the $TWEEN_{extract}$ were strongly correlated (~0.95) with the concentration of DWCNTs. Moreover, the amount of PLPs extracted for each condition increased according to the concentration of DWCNTs. In contrast, the concentration of carbohydrates from the $TWEEN_{extract}$ was significantly higher only at the highest concentration of DWCNTs. As already observed with polystyrene nanoparticles [60], our results suggest a strong hydrophobic interaction between DWCNTs and EPS, which is mainly driven by PLPs. These results corroborate the HPLC results, which showed increases in two PLPs (~174 kDa, ~10 kDa) that could be strongly implicated in the observed hydrophobic interaction between EPS and DWCNTs. Tyrosine and tryptophan, which are cyclic amino acids, are especially involved in the CNTs-protein interaction [61]. This indicates that these two PLPs could contain a large amount of these two amino acids. In addition, the sharp increase in the protein/carbohydrates ratio of EPS in the exposed cultures appears to be an adaptive/adhesive response of N. palea that works by increasing the hydrophobicity of the EPS produced. EDTA was used to chelate ions responsible for the ionic bridge between DWCNTs and EPS, allowing for their extraction. The $EDTA_{extract}$ (Fig. 4c) revealed no

significant difference between conditions, although the amount extracted showed an increasing trend following that of DWCNTs. Thus, the involvement of ionic bonds was weak but they cannot be ruled out in the binding of DWCNTs to EPS. Structural defects in DWCNTs might be implicated in this type of interaction, and replicating the experiment using functionalized DWCNTs would better help us to grasp the potential of EPS to form ionic bonds with DWCNTs. NOM could also be involved in the interaction observed between EPS and DWCNTs either by reducing or promoting it. On the one hand, NOM can occupy hydrophobic areas that are inherent to DWCNTs, limiting interaction between DWCNTs and EPS [64]. On the other hand, NOM could promote the interaction between DWCNTs and EPS through forming different bonds such as electrostatic, hydrophobic, π–π and hydrogen-bond interactions [17,63] with both DWCNTs and EPS [17,50].

Due to the nano-particulate and fibrous nature of the DWCNTs as well as the structure of the EPS network, a mechanical interaction seems obvious. This is supported by SEM observations showing DWCNTs strongly entangled in the EPS (Fig. 5). According to other authors, the assembly of DWCNTs and EPS is consistent with them encountering each other within a few seconds [62] and occurs even under dynamic water flow, as in the used experimental setup. In the present study, a strong disruption in the EPS structure was also highlighted, which was already observed during the exposure of human mucus to MWCNTs [27] using other non-metallic nanoparticles [54]. This disruption could be a consequence of both mechanical phenomena and chemical interactions (mainly hydrophobic, Figs. 4b and 5c) between different EPS polymers and DWCNTs. This could increase the coating and retention of DWCNTs within the EPS that compose aquatic biofilms.

5. Conclusion

Exposure to 1–50 mg L^{-1} of DWCNTs dispersed by NOM led to a temporary growth inhibition of the diatom N. palea. However, no toxic effect was observed in either the viability or the PSII quantum yield. Shading seemed involved only in growth inhibition from DWCNTs[10mg], although the device used in the present study is believed to underestimate the shading effect at low concentrations of CNT. The EPS analysis revealed a DWCNT-driven overproduction of EPS from DWCNTs[1mg]. This was specifically the case for PLPs but not for carbohydrate polymers. Overproduction was stable for DWCNTs[1mg] to DWCNTs[10mg], indicating a strong response from low DWCNT concentrations. An additive effect of shading and energetic trade-off between cell division and EPS production (focused on protection against DWCNTs) could explain the observed growth inhibition after 48 h of contact.

This study has also shown that two distinct mechanisms were involved in the interaction between DWCNTs and EPS: (i) physical, via the EPS meshing, and (ii) chemical, mainly via hydrophobic interactions. Two PLPs seemed particularly involved in the latter but further studies are needed to better characterize the implicated molecules and understand the basics of the interaction. In general, our results show that EPS production by N. palea could be a general response to

stress from both natural particles (clays and sediments) and anthropogenic particles (manufactured nanoparticles). However, it is unlikely that EPS production is changed similarly for algae under shading conditions and DWCNTs exposure. This might be confirmed by an additional study on EPS production, making the distinction between the role of direct interactions (contact between DWCNTs and diatoms) and the shading caused by DWCNTs.

However, considering that the present and future concentrations of CNTs in aquatic environments are low in comparison to those of natural particles, only a minor impact of CNTs on EPS production at a worldwide scale is foreseen. In contrast, the covering of CNTs by EPS and probably by other hydrophobic nanoparticles could hide them from the recognition and defense systems of many organisms. Thus, EPS-coated nanoparticles could become Trojans overlooked by many organisms that consume the biofilms.

Declaration of interest

Acknowledgments

Appendix A. Supplementary data

Supplementary data associated with this article can be found, in the online version, at http://dx.doi.org/10.1016/j.carbon.2015.02.053.

REFERENCES

[1] Carbon nanotubes (CNTs) market by type (SWCNTS & MWCNTS), application (electronics & semiconductors, chemical & polymers, batteries & capacitors, energy, medical, composites, & aerospace & defense) & geography – global trends & forecasts to 2018; MarketsandMarkets publisher. 2013.

[2] Production and applications of carbon nanotubes, carbon nanofibers, fullerenes, graphene and nanodiamonds: a global technology survey and market analysis. Innovative Research and Products (iRAP), Inc, 2011.

[3] Flahaut E, Bacsa R, Peigney A, Laurent C. Gram-scale CCVD synthesis of double-walled carbon nanotubes. Chem Commun 2003:1442. http://dx.doi.org/10.1039/b301514a.

[4] Endo M, Strano MS, Ajayan PM. Potential applications of carbon nanotubes. Carbon Nanotubes, vol. 111. Berlin, Heidelberg: Springer Berlin Heidelberg; 2008 [p. 13–61].

[5] Béduer A, Seichepine F, Flahaut E, Loubinoux I, Vaysse L, Vieu C. Elucidation of the role of carbon nanotube patterns on the development of cultured neuronal cells. Langmuir 2012;28:17363–71. http://dx.doi.org/10.1021/la304278n.

[6] Neves V, Heister E, Costa S, Tîlmaciu C, Flahaut E, Soula B, et al. Design of double-walled carbon nanotubes for biomedical applications. Nanotechnology 2012;23:365102. http://dx.doi.org/10.1088/0957-4484/23/36/365102.

[7] Petersen EJ, Zhang L, Mattison NT, O'Carroll DM, Whelton AJ, Uddin N, et al. Potential release pathways, environmental fate, and ecological risks of carbon nanotubes. Environ Sci Technol 2011;45:9837–56. http://dx.doi.org/10.1021/es201579y.

[8] Kümmerer K, Menz J, Schubert T, Thielemans W. Biodegradability of organic nanoparticles in the aqueous environment. Chemosphere 2011;82:1387–92. http://dx.doi.org/10.1016/j.chemosphere.2010.11.069.

[9] Parks AN, Chandler GT, Ho KT, Burgess RM, Ferguson PL. Environmental biodegradability of [^{14}C]SWNT by Trametes versicolor and natural microbial cultures found in New Bedford Harbor sediment and aerated wastewater treatment plant sludge: environmental biodegradability of [^{14}C]SWNT. Environ Toxicol Chem 2014:n/a–a. http://dx.doi.org/10.1002/etc.2791.

[10] Zhang L, Petersen EJ, Habteselassie MY, Mao L, Huang Q. Degradation of multiwall carbon nanotubes by bacteria. Environ Pollut 2013;181:335–9. http://dx.doi.org/10.1016/j.envpol.2013.05.058.

[11] Smart SK, Cassady AI, Lu GQ, Martin DJ. The biocompatibility of carbon nanotubes. Carbon 2006;44:1034–47. http://dx.doi.org/10.1016/j.carbon.2005.10.011.

[12] Petersen EJ, Henry TB. Methodological considerations for testing the ecotoxicity of carbon nanotubes and fullerenes: review. Environ Toxicol Chem 2012;31:60–72. http://dx.doi.org/10.1002/etc.710.

[13] Wick P, Manser P, Limbach L, Dettlaffweglikowska U, Krumeich F, Roth S, et al. The degree and kind of agglomeration affect carbon nanotube cytotoxicity. Toxicol Lett 2007;168:121–31. http://dx.doi.org/10.1016/j.toxlet.2006.08.019.

[14] Wei L, Thakkar M, Chen Y, Ntim SA, Mitra S, Zhang X. Cytotoxicity effects of water dispersible oxidized multiwalled carbon nanotubes on marine alga *Dunaliella tertiolecta*. Aquat Toxicol 2010;100:194–201. http://dx.doi.org/10.1016/j.aquatox.2010.07.001.

[15] Schwab F, Bucheli TD, Lukhele LP, Magrez A, Nowack B, Sigg L, et al. Are carbon nanotube effects on green algae caused by shading and agglomeration? Environ Sci Technol 2011;45:6136–44. http://dx.doi.org/10.1021/es200506b.

[16] Navarro E, Baun A, Behra R, Hartmann NB, Filser J, Miao A-J, et al. Environmental behavior and ecotoxicity of engineered nanoparticles to algae, plants, and fungi. Ecotoxicology 2008;17:372–86. http://dx.doi.org/10.1007/s10646-008-0214-0.

[17] Yang K, Xing B. Adsorption of fulvic acid by carbon nanotubes from water. Environ Pollut 2009;157:1095–100. http://dx.doi.org/10.1016/j.envpol.2008.11.007.

[18] Zhang S, Shao T, Kose HS, Karanfil T. Adsorption kinetics of aromatic compounds on carbon nanotubes and activated carbons. Environ Toxicol Chem 2012;31:79–85. http://dx.doi.org/10.1002/etc.724.

[19] Bourdiol F, Mouchet F, Perrault A, Fourquaux I, Datas L, Gancet C, et al. Biocompatible polymer-assisted dispersion of multi walled carbon nanotubes in water, application to the investigation of their ecotoxicity using *Xenopus laevis* amphibian larvae. Carbon 2013;54:175–91. http://dx.doi.org/10.1016/j.carbon.2012.11.024.

[20] Staats N, De Winder B, Stal L, Mur L. Isolation and characterization of extracellular polysaccharides from the epipelic diatoms *Cylindrotheca closterium* and *Navicula salinarum*. Eur J Phycol 1999;34:161–9. http://dx.doi.org/10.1080/09670269910001736212.

[21] Tolhursf TJ, Gust G, Paterson DM. The influence of an extracellular polymeric substance (EPS) on cohesive sediment stability. Proc Mar Sci 2002;5:409–25.

[22] Brouwer JFC, Wolfstein K, Ruddy GK, Jones TER, Stal LJ. Biogenic stabilization of intertidal sediments: the importance of extracellular polymeric substances produced by benthic diatoms. Microb Ecol 2005;49:501–12. http://dx.doi.org/10.1007/s00248-004-0020-z.

[23] Flemming HC, Wingender J. Relevance of microbial extracellular polymeric substances (EPSs) – Part I: structural and ecological aspects. Water Sci Technol J Int Assoc Water Pollut Res 2001;43:1–8.

[24] Riding RE, Awramik SM, editors. Microbial sediments. Berlin, Heidelberg: Springer Berlin Heidelberg; 2000.

[25] De Brouwer JFC, Stal LJ. Daily fluctuations of exopolymers in cultures of the benthic diatoms *Cylindrotheca closterium* and *Nitzschia* sp. (Bacillariophyceae). J Phycol 2002;38:464–72. http://dx.doi.org/10.1046/j.1529-8817.2002.01164.x.

[26] Miao A-J, Schwehr KA, Xu C, Zhang S-J, Luo Z, Quigg A, et al. The algal toxicity of silver engineered nanoparticles and detoxification by exopolymeric substances. Environ Pollut 2009;157:3034–41. http://dx.doi.org/10.1016/j.envpol.2009.05.047.

[27] Verneuil L, Silvestre J, Mouchet F, Flahaut E, Boutonnet J-C, Bourdiol F, et al. Multi-walled carbon nanotubes, natural organic matter, and the benthic diatom *Nitzschia palea*: "A sticky story". Nanotoxicology 2014:1–11. http://dx.doi.org/10.3109/17435390.2014.918202.

[28] Scala S, Bowler C. Molecular insights into the novel aspects of diatom biology. Cell Mol Life Sci 2001;58:1666–73. http://dx.doi.org/10.1007/PL00000804.

[29] Hamm CE, Merkel R, Springer O, Jurkojc P, Maier C, Prechtel K, et al. Architecture and material properties of diatom shells provide effective mechanical protection. Nature 2003;421:841–3. http://dx.doi.org/10.1038/nature01416.

[30] Losic D, Rosengarten G, Mitchell JG, Voelcker NH. Pore Architecture of diatom frustules: potential nanostructured membranes for molecular and particle separations. J Nanosci Nanotechnol 2006;6:982–9. http://dx.doi.org/10.1166/jnn.2006.174.

[31] Debenest T, Silvestre J, Coste M, Pinelli E. Effects of pesticides on freshwater diatoms. In: Whitacre DM, editor. Reviews of environmental contamination and toxicology volume 203, vol. 203. New York, NY: Springer; 2010. p. 87–103.

[32] Landois P. Synthèse, fonctionnalisation et impact sur l'environnement de nanotubes de carbone. Toulouse: Centre Interuniversitaire de la Recherche et d'Ingénierie des Matériaux (CIRIMAT), UMR 5085; Laboratoire D'Ecologie fonctionnelle et environnement (EcoLab), UMR 5245; 2008.

[33] Oeurng C, Sauvage S, Coynel A, Maneux E, Etcheber H, Sánchez-Pérez J-M. Fluvial transport of suspended sediment and organic carbon during flood events in a large agricultural catchment in southwest France. Hydrol Processes 2011;25:2365–78. http://dx.doi.org/10.1002/hyp.7999.

[34] Horst AM, Vukanti R, Priester JH, Holden PA. An assessment of fluorescence- and absorbance-based assays to study metal-oxide nanoparticle ROS production and effects on bacterial membranes. Small 2013;9:1753–64. http://dx.doi.org/10.1002/smll.201201455.

[35] Ras M, Lefebvre D, Derlon N, Paul E, Girbal-Neuhauser E. Extracellular polymeric substances diversity of biofilms grown under contrasted environmental conditions. Water Res 2011;45:1529–38. http://dx.doi.org/10.1016/j.watres.2010.11.021.

[36] Dreywood R. Qualitative test for carbohydrate material. Ind Eng Chem Anal Ed 1946;18:499. http://dx.doi.org/10.1021/i560156a015.

[37] Smith PK, Krohn RI, Hermanson GT, Mallia AK, Gartner FH, Provenzano MD, et al. Measurement of protein using bicinchoninic acid. Anal Biochem 1985;150:76–85.

[38] Cleuvers M, Ratte HT. The importance of light intensity in algal tests with coloured substances. Water Res 2002;36:2173–8. http://dx.doi.org/10.1016/S0043-1354(01)00455-9.

[39] Oecd O. Guidance document on aquatic toxicity testing of difficult substances and mixtures. Paris, France: OECD Publishing; 2002.

[40] Youn S, Wang R, Gao J, Hovespyan A, Ziegler KJ, Bonzongo J-CJ, et al. Mitigation of the impact of single-walled carbon nanotubes on a freshwater green algae: *Pseudokirchneriella subcapitata*. Nanotoxicology 2012;6:161–72. http://dx.doi.org/10.3109/17435390.2011.562329.

[41] Ge C, Li Y, Yin J-J, Liu Y, Wang L, Zhao Y, et al. The contributions of metal impurities and tube structure to the toxicity of carbon nanotube materials. NPG Asia Mater 2012;4:e32. http://dx.doi.org/10.1038/am.2012.60.

[42] Von Moos N, Slaveykova VI. Oxidative stress induced by inorganic nanoparticles in bacteria and aquatic microalgae – state of the art and knowledge gaps. Nanotoxicology 2013:1–26. http://dx.doi.org/10.3109/17435390.2013.809810.

[43] El-Sheekh MM, El-Naggar AH, Osman MEH, El-Mazaly E. Effect of cobalt on growth, pigments and the photosynthetic electron transport in *Monoraphidium minutum* and *Nitzschia perminuta*. Braz J Plant Physiol 2003;15. http://dx.doi.org/10.1590/S1677-04202003000300005.

[44] Nagpal NK, Golder Associates, British Columbia, Ministry of Water Land AP. Technical report, water quality guidelines for cobalt. Victoria, B.C.: Ministry of Water, Land and Air Protection; 2004.

[45] Canadian Council of Ministers of the Environment. Canadian environmental quality guidelines. Hull, QC: CCME; 1999.

[46] Khandeparker RD, Bhosle NB. Extracellular polymeric substances of the marine fouling diatom *Amphora rostrata* Wm. Sm. Biofouling 2001;17:117–27. http://dx.doi.org/10.1080/08927010109378471.

[47] Takahashi E, Ledauphin J, Goux D, Orvain F. Optimising extraction of extracellular polymeric substances (EPS) from benthic diatoms: comparison of the efficiency of six EPS extraction methods. Mar Freshw Res 2009;60:1201. http://dx.doi.org/10.1071/MF08258.

[48] Underwood GJC, Boulcott M, Raines CA, Waldron K. Environmental effects on exopolymer production by marine benthic diatoms: dynamics, changes in composition, and pathways of production. J Phycol 2004;40:293–304. http://dx.doi.org/10.1111/j.1529-8817.2004.03076.x.

[49] Chen Y-P, Zhang P, Guo J-S, Fang F, Gao X, Li C. Functional groups characteristics of EPS in biofilm growing on different carriers. Chemosphere 2013;92:633–8. http://dx.doi.org/10.1016/j.chemosphere.2013.01.059.

[50] Stal LJ. Microphytobenthos, their extracellular polymeric substances, and the morphogenesis of intertidal sediments. Geomicrobiol J 2003;20:463–78. http://dx.doi.org/10.1080/713851126.

[51] Poulíčková A, Hašler P, Lysáková M, Spears B. The ecology of freshwater epipelic algae: an update. Phycologia 2008;47:437–50. http://dx.doi.org/10.2216/07-59.1.

[52] Joshi N, Ngwenya BT, French CE. Enhanced resistance to nanoparticle toxicity is conferred by overproduction of extracellular polymeric substances. J Hazard Mater 2012;241–242:363–70. http://dx.doi.org/10.1016/j.jhazmat.2012.09.057.

[53] Hessler CM, Wu M-Y, Xue Z, Choi H, Seo Y. The influence of capsular extracellular polymeric substances on the interaction between TiO_2 nanoparticles and planktonic bacteria. Water Res 2012;46:4687–96. http://dx.doi.org/10.1016/j.watres.2012.06.009.

[54] Wang Y-Y, Lai SK, So C, Schneider C, Cone R, Hanes J. Mucoadhesive nanoparticles may disrupt the protective human mucus barrier by altering its microstructure. PLoS One 2011;6:e21547. http://dx.doi.org/10.1371/journal.pone.0021547.

[55] Smith DJ, Underwood JC. Exopolymer production by intertidal epipelic diatoms. Limnol Oceanogr 1998;7:1578–91.

[56] Wolfstein K, Stal L. Production of extracellular polymeric substances (EPS) by benthic diatoms: effect of irradiance and temperature. Mar Ecol Prog Ser 2002;236:13–22. http://dx.doi.org/10.3354/meps236013.

[57] Caudan C, Filali A, Lefebvre D, Spérandio M, Girbal-Neuhauser E. Extracellular polymeric substances (eps) from aerobic granular sludges: extraction, fractionation, and anionic properties. Appl Biochem Biotechnol 2012;166:1685–702. http://dx.doi.org/10.1007/s12010-012-9569-z.

[58] Long Z, Ji J, Yang K, Lin D, Wu F. Systematic and quantitative investigation of the mechanism of carbon nanotubes' toxicity toward algae. Environ Sci Technol 2012;46:8458–66. http://dx.doi.org/10.1021/es301802g.

[59] Johnson M. Detergents: triton X-100, tween-20, and more. Mater Methods 2013;3. http://dx.doi.org/10.13070/mm.en.3.163.

[60] Chen C-S, Anaya JM, Zhang S, Spurgin J, Chuang C-Y, Xu C, et al. Effects of engineered nanoparticles on the assembly of exopolymeric substances from phytoplankton. PLoS One 2011;6:e21865. http://dx.doi.org/10.1371/journal.pone.0021865.

[61] Mu Q, Jiang G, Chen L, Zhou H, Fourches D, Tropsha A, et al. Chemical basis of interactions between engineered nanoparticles and biological systems. Chem Rev 2014. http://dx.doi.org/10.1021/cr400295a [140613144559008].

[62] Tenzer S, Docter D, Kuharev J, Musyanovych A, Fetz V, Hecht R, et al. Rapid formation of plasma protein corona critically affects nanoparticle pathophysiology. Nat Nanotechnol 2013;8:772–81. http://dx.doi.org/10.1038/nnano.2013.181.

[63] Zhou X, Shu L, Zhao H, Guo X, Wang X, Tao S, et al. Suspending multi-walled carbon nanotubes by humic acids from a peat soil. Environ Sci Technol 2012;46:3891–7. http://dx.doi.org/10.1021/es204657k.

[64] Edgington AJ, Roberts AP, Taylor LM, Alloy MM, Reppert J, Rao AM, et al. The influence of natural organic matter on the toxicity of multiwalled carbon nanotubes. Environ Toxicol Chem 2010;29:2511–8. http://dx.doi.org/10.1002/etc.309.